Evolutionary Dimensionality Reduction for Crack Localization in Ship Structures using a Hybrid Computational Intelligent Approach

Vassilios A. Kappatos, George Georgoulas, Chrysostomos D. Stylios, and Evangelos S. Dermatas

Abstract—**Acoustic Emission (AE) is one of the most important Non-Destructive Testing (NDT) methods for materials and constructions. Using AE testing, the location of a single event (crack) can be classified efficiently into three typical areas in a ship hull. The problem is a typical classification problem based on the use of features extracted from piezo-sensors' signal. As in most classification problems, the extraction and selection of the most appropriate set of features plays a major role in the overall performance of the system. In this research work we investigate the use of an evolutionary algorithm to extract new features from a set of primitive features in a lower dimensional space through a linear transformation. These features are subsequently fed into a Probabilistic Neural Network (PNN) that performs the classification. In simulation experiments, where a Stiffened Plate Model (SPM) is partially sank into water, the localization rate in noisy environments outperforms a recent work, where a feature selection phase alone was used before the classification phase. The proposed hybrid computational intelligent approach shows the potential merit of using it in real life situations where the signal is distorted by noise.**

I. Introduction

One of the most well known and successful NDT methods for the detection and location of cracks in a variety of metal structures is Acoustic Emission (AE). AE is the implementation of a transient wave resulting from sudden release of stored energy during a deformation failure process such as a crack, multiple dislocation slips, twinning, grain boundary sliding, leaks, structural vibrations, electrical transients etc. The processing of AE signals is based on the detection and conversion of elastic waves to electrical signals by directly coupling piezoelectric transducers on the surface of the structure under examination. AE is sensitive enough to detect newly formed crack surfaces down to a few hundred square micrometers and less. The interested reader can find more information about AE and NDT methods in [1] and [2].

V. A. Kappatos is with the Electrical Engineering Department, University of Patras, 26500, Rio, Patra, Hellas (corresponding author to provide phone: +30-2610-996189; fax: +30-2610-996189; e-mail: kappatos@george.wcl2.ee.upatras.gr).

G. Georgoulas is with the Dept of Computer Applications in Finance and Management, TEI of Ionian Islands, Lefkas, Greece (e-mail: georgoul@teiion.gr).

C. D. Stylios is with the Laboratory of Knowledge and Intelligent Computing, Dept. of Informatics and Communications Technology, TEI of Epirus, 47100 Artas, Greece (email: stylios@teiep.gr)

E. S. Dermatas is with the Electrical Engineering Department, University of Patras, 26500, Rio, Patra, Hellas (e-mail: dermatas@george.wcl2.ee.upatras.gr).

Corrosion and fatigue cracking are the most pervasive types of structural problems present in ship structures. These damage modes, if not properly monitored and rectified, could potentially lead to catastrophic failure or unanticipated out-of-service time. Especially for the case of a ship, which transports crude oil, the consequence of an oil spill due to a broken weld would be disastrous. Therefore the ship inspection for structural reliability is of critical concern. Existing techniques for the inspection of ship structures require them to be taken out of service and one must keep in mind that ships' downtime is costly. A technique that can detect damage while the ship is in normal operation is greatly desired, while the identification of the extent and the location of the damage is an even more complex problem.

Numerous analytical and experimental approaches to investigate fatigue damage occurrence in ships have been proposed in recent years. A considerable amount of all fatigue damage in ship hulls occurs in the side shell plating, especially at the connection between longitudinal and heavy transverse parts, as reported in [3] and [4]. Five full-scale specimens representing side longitudinal of floating production storage and offloading units were fatigue tested in [5]. The connections were very similar to connections currently in use, and they were fabricated according to typical ship-yard practice. The specimens were also modelled by finite elements and some of the results from the most complex connections have been compared with measured data.

Soares et al [6] presented a theoretical formulation for the assessment of the reliability of a ship hull with respect to fatigue failure of the longitudinal members. The model allows for multiple cracks both in the side longitudinal and in the side shell and it models the crack growth process.

Usually, the dynamic characteristics of the structure change when structural damage occurs. Zybaydi et al. proposed an autocorrelation function to identify damage in the side shell of ship structures using a combination of experimental and numerical studies [7]. The damage occurrence in the side shell of ship structures, modelled as a stiffened plate, was identified using the random decrement technique. Zubaydi et al. [8] also proposed a Neural Network (NN) technique to identify the damages in the side shell of a ship's structure where the autocorrelation function of the structure vibration response was the input to the NN. The theoretical response was obtained using a finite element model of the structure.

The selection and identification of the best feature set is a complicated problem and the optimum solution is currently an open issue in pattern recognition literature [9], [10].

978-1-4244-3553-1/09/$25.00 ©2009 IEEE

Robust detection of crack signals in noisy environments improves significantly the reliability of real-time monitoring systems in adverse weather conditions, in large and complex constructions. A recent feature selection method based on the *K*-means clustering algorithm and the Principal Component Analysis (PCA) [11] was used to define a small and robust set of features for this specific application. Thus, the localization of AE sources was achieved using a small set of features decreasing significantly the memory requirements and the computational complexity. Both methods exploit the internal structure of the feature space neglecting the labelling information available.

This paper presents an efficient algorithm for automatic and real-time localization of AE events using a robust set of features "constructed" through a linear transformation of a set of primitive features. The class information is used in the features extraction problem, maximizing the correct classification rate of a Probabilistic Neural Network (PNN) "closing the loop" between the features selection step and the classification.

Usually evolutionary algorithms are employed as a means to select relevant features from a larger set of "primitive" features [12]. In this research work we employ an evolutionary approach to "project" the features in a lower dimensional space which maximizes the classification performance. At the same time the evolutionary algorithm "optimizes" the spread of the Gaussian functions of the PNN.

In normal ship operation, real-life noise sources, i.e. engines, waves, weather conditions etc., reduce significantly the capability of localization and characterization of crack events. For this reason, the evaluation process is carried out in the presence of white Gaussian noise added at 20 to -20 dB SNR.

The rest of the paper is organized as follows: Section II presents the experimental structure, which was used to test a metal structure and the data acquisition system. Section III gives a detailed description of the relevant background for the localization of AE sources based on computational intelligence techniques. Section IV describes the experimental data and the results using the proposed method and Section V concludes the paper and gives directions for future work.

II. Experimental Setup

A stiffened plate was used to model the side shell of a ship structure. The structure and dimensions of the SPM are shown in Fig. 1. The outside side shell was dyed with oil-paint in order to simulate as closely as possible the ship's outer side.

Reflections at the end of the SPM were reduced by wrapping the ends in putty. In order to investigate the influence of water, the SPM and its supports were fixed in a water tank, as shown in Fig. 2. The putty at the edges of the SPM prevents water from passing in the inside side shell of the plate. The putty was dyed with oil-paint for better water-tightness and also to prevent putty corrosion.

The fixed boundary condition of the model was obtained by clamping the side shell by three heavy bases. Insulation material was placed between: a) the SPM and the three bases, b) the three bases and the bottom of the tank, and c) the bottom of the tank and the floor to eliminate external noise.

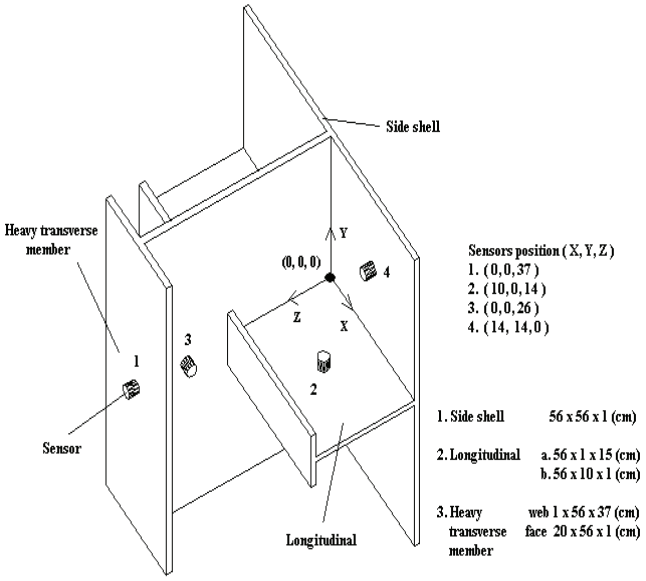

Fig. 1. The stiffened plate under test along with the sensors' positions.

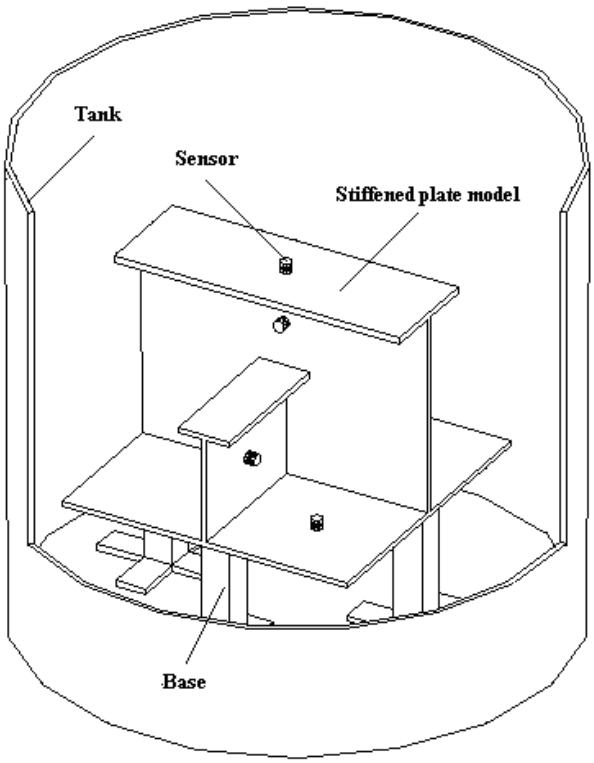

Fig. 2. The tank with the stiffened plate model under test.

To detect the wave in the steel stiffened plate, the Physical Acoustics Corporation (PAC) R15-Alpha sensors were used. The sensors were stuck on the plate with grease-couplant. In real life applications, where the installation cost is a significant factor, the number of sensors must be kept low and at the same time the sensors must be regulated at maximum sensitivity to cover a great ship-hull area. In our experiments, the pulser amplitude was decreased, and the gain was set on the specification limits of the amplifiers used. This setting closely resembles a real-life application, where the received signal propagates at several adjacent stiffened plates and the signal reflection at the plate edges is minimized. The sensors' signal was correspondingly amplified at 58dB (two sensors), 70.7dB and 80dB, digitized at 1MHz with 16 bit accuracy and stored in the AE analysis system PAC Mistras 2001. The four channel's AE system was triggered, when the signal on any channel exceeded a pre-defined threshold, and the four-channel simultaneous recordings were stored in a hard-disk. The AE source was simulated with a Piezoelectric Pulse-Generator (PPG), which is a common practice [15].

In order to detect the AE-signal arriving from any possible position, the four sensors were set in symmetrical positions, taking into account the structure of the ship-hull. The first, the second and the third sensors were located in the middle of the face plate of the heavy/longitudinal/side shell respectively, minimizing the total distance between the welding seam points and the nearest sensor. The fourth sensor was located in the middle of the distance between the heavy transverse face and the faceplate of longitudinal. In Fig. 2, the exact arrangement of the sensors is shown.

The studies by Strathaus et al. [3] and Sucharski [4] have shown that fatigue due to wave-induced loads is the main cause of ship structural damage, especially for structures having high stress concentrations at the connection between the longitudinal and the heavy transverse members of the side shell.

III. Localization of AE Sources in Ship Hulls

In this research work, we propose a method for AE-source localization, which consists of three modules: the feature extraction module, where a set of primitive features is derived from the AE signal, the evolutionary algorithm used to construct new features from the primitive set and finally the PNN detector that locates the area of the AE source. The second and third modules are strongly coupled since the PNN is "optimized" via the evolutionary algorithm and since the classification performance guides the evolutionary search.

A. Feature Extraction

In a typical data recording system of AE signals, the acquired samples (simultaneous signals from multiple installed piezoelectric sensors) are recorded, when the channel amplitude exceeds a manually pre-defined threshold. A set of N features from each signal is estimated. Therefore, a total number of MxN features are available when the system acquires one AE event where M is the number of installed sensors.

Recently Kappatos et al., [11] presented an extensive study on the feature selection problem for robust detection of AE-signals in raining conditions, where a total number of ninety features were extracted, sixty seven in the time domain and twenty three in the frequency domain. The forty nine are primitive features, derived directly from the AE signal, and the rest forty-one consist of non-linear transformations of the primitive features in either time or frequency domain. In this paper the same features are used to derive the most effective features as presented in the following section.

B. Evolutionary Dimensionality Reduction

Dimensionality reduction can either be performed through feature selection or through transformation/mapping of the original vector to a lower dimensional space. In fact the proposed algorithm is a member of the latter class where the mapping is a linear (and sparse) one. In any case the main purpose of feature selection is to reduce the number of features without compromising the classification performance. Moreover, sometimes the elimination of less discriminatory features increases the generalization capabilities of the classification method [10]. Especially in situations where the number of available data is limited and comparable to the number of the features, the curse of dimensionality leads to overtraining effects in the training process of the classifier.

A very popular approach to dimensionality reduction is to apply a linear transformation of the original feature vectors. In other words, given an nxd pattern matrix A (n training data of dimension d) come up with a reduced pattern matrix B with dimensions nxm with $m<d$. This transformation is performed through a transformation matrix H (dxm):

$$B = A \cdot H \tag{1}$$

Different transformation matrices can be produced entirely in a deterministic manner based on the selected method and the corresponding optimization criterion.

On the other hand, Raymet et al. [13], proposed a genetic algorithm (GA) to come up with a sparse matrix with only one nonzero entry in each column of the H matrix. This method selects features from the original set and scales them by an "appropriate" weight, eliminating at the same time features that do not contribute to classification performance. Therefore, they have created a wrapper [9] with the classifier being a k-nearest neighbor ($k$nn) with a genetically selected number of neighbors. In [14], a GA is used to select among the eigenvectors of the covariance matrix that are subsequently used for the projection of the original data. This wrapper approach based on the classification error, guides the selection of the retained eigenvectors in contrast to the popular "minimization of the retained variance" approach (filter approach).

In this paper, an evolutionary algorithm is used to estimate the matrix H for a predefined number of columns (m), i.e. a predefined number of "constructed" features. Instead of using predefined directions derived from a PCA stage, as in [14] or just using the sparse matrix of [13] we propose the construction of matrix H using a real valued GA.

The GA population consists of real valued chromosomes divided into five competing subpopulations [16]. Each of the subpopulations competes for more resources with the one having the best performance given a greater number of chromosomes/individuals. Each subpopulation has a different range of the mutation rate leading to different degrees of search space exploration [17].

The reallocation of resources is performed every four generations. Only the best subpopulation receives recourses (the worst individuals from the less successful subpopulations are transferred to the best subpopulation). The number of individuals per subpopulation cannot fall bellow five and the number of resources transferred each time is set equal to 0.1 of the total number of individuals (the resource consumption for each individual is one). The share of recourses of each subpopulation is based on linear ranking (with a selection pressure set to 2) [16].

For the selection process, stochastic universal sampling was employed with selection pressure equal to 1.7 [18]. Recombination ("crossover") was performed using discrete recombination [16], [19] with the recombination rate set equal to 1. Mutation was performed by adding randomly (uniformly) created values to the variables [16], [19]. The mutation rate was set to $1/n$ (where n is the number of variables-genes) [19] and the mutation range for each one of the subpopulations (numbering 50, 30, 30, 20 and 10 individuals respectively) was set to 0.1, 0.03, 0.01, 0.003, 0.001. The GA was implemented using the GEATBx toolbox [16] and was let to run for 250 "generations".

Since we have ninety features in total, each projection direction needs ninety genes to encode the corresponding weights. We have to mention that in our approach each feature is not related to the corresponding sensor. This means that the same transformation is applied to the same feature estimated from the signal acquired at different sensors. If we had treated each sensor separately this would have lead to a total of 360 features. Apart from the genes reserved to encode the entries of the H matrix, we also genetically encode the spread σ of the PNN, as described in the following section.

C. Probabilistic Neural Network (PNN)

A PNN consists of d input features, n pattern units and c class units, as shown in Fig. 3.

Each pattern unit forms the inner product of its weight vector $\mathbf{w}$ and the normalized input vector $\mathbf{x}$, $z = \mathbf{w}^T\mathbf{x}$. The nonlinear activation function of $f(z) = \exp\left((z-1)/\sigma^2\right)$ is used to transform the inner product and σ is a parameter determined by the user which defines how smooth the decision surface will be. The neuron outputs are accumulated and the corresponding class unit produces the probability of the input vector to belong to each one of the c classes.

"Training" of a PNN (i.e. setting the weights equal to the normalized - $\|\mathbf{x}\| = 1$ - training patterns) can be very fast, compensating this way for the time consuming process of the evolutionary algorithm (which also "tunes" the parameter σ).

IV. Data Set and Results

In this research work we conducted a number of experiments, using the experimental structure which was presented in Section II, to tackle the problem of AE source localization in ship structures. To be more specific the AE feature-vector is classified in one among three classes, listed bellow:

1. AE source in the welding seam between the longitudinal and the heavy transverse member (web) (class-A),
2. AE source in the welding seam between the longitudinal and the side shell (class-B),
3. AE source in the welding seam between the heavy transverse member (web) and side shell (class-C).

Data for each class (A, B, C), were generated at 90 different positions almost uniformly distributed in the welding-seam areas. At each position, the pulser is triggered five times to simulate the signal variance of AE events at the same position.

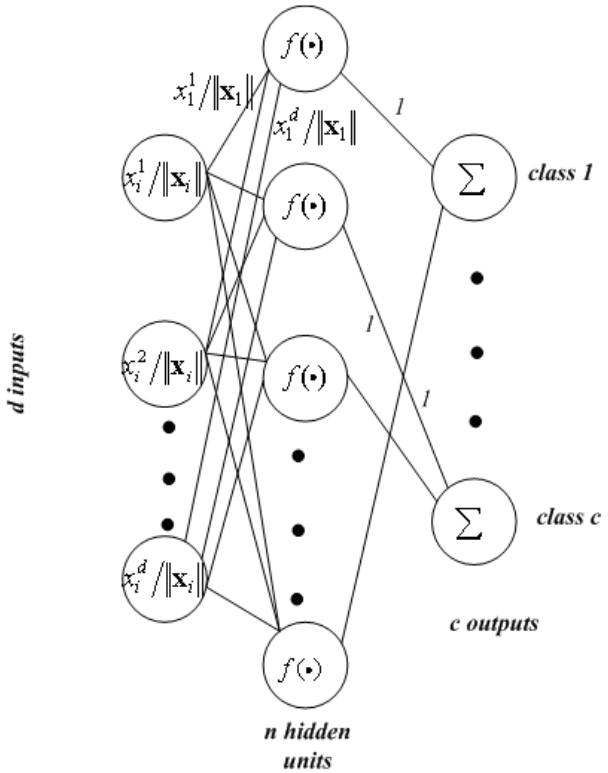

Fig. 3. Graphical representation of the PNN structure.

In Table 1 the number of cases (data points) investigated

for each class and for each one of the 6 noise levels that were tested, is shown.

TABLE I
CASES EMPLOYED IN THE STUDY

	Class A	Class B	Class C
Noise free	144	113	124
20 dB	141	124	110
10 dB	139	110	122
0 dB	137	108	119
-10 dB	150	119	121
-20 dB	184	137	148

In order to evaluate our approach, the available data are split into 3 sets:

1. A training set that contains 60% of the available data
2. A validation set (20%), and
3. A testing set (20%)

The assignment of each data point to one of the aforementioned sets was performed randomly. The training and validations sets were used to perform the feature selection phase and to tune the spread parameter of the PNN. Once the *H* matrix was constructed and the spread was selected via the GA, the train and the validation sets were merged to form the new train set and were used to train the PNN, which was subsequently tested using the testing set. This type of evaluation estimates the classification accuracy using cases that hadn't been used in any of the training phases, leading to a minimal biased estimation of the mean accuracy [20]. In order to account for the stochastic nature of the evolutionary algorithm have repeated each experiment 5 times.

As mentioned in the previous section we conducted a set of experiments to validate the discrimination capabilities of our approach. The underlying idea was to derive a set of "global" projection directions to transform the data. By the term "global" we mean that the same direction was used for all feature vectors (each sensor gives rise to a 90-dimensional feature vector). In other words when we are talking about four projected features we actually had 4x4=16 features in the PNN input (the same four directions for each one of the four sensors). Moreover, the proposed AE localization method was evaluated in the presence of white Gaussian noise with zero mean value at -20, -10, 0, 10, 20dB SNR, allowing for an interesting study in the feature definition problem in noisy signals.

We tried to use one and up to four projection directions and the results for the best configurations are summarized in Table II. In the appendix, the mean Confusion Matrices for each one configuration are presented.

In the noise-free case and the high SNRs, the number of selected projection dimensions doesn't significantly affect the classification accuracy. On the other hand for higher noise levels, the selection of just one projection direction is the preferred choice.

Compared to our previous work [12], where a binary Particle Swarm Optimization (bPSO) was employed to select features using the same set of ninety features and a Multilayer Perceptron (MLP) neural network, the current approach performs better in the presence of noise. To be more specific, for only one feature the current approach is superior for the case of -10 dB and almost the same rate is achieved in case of 0 dB. On the other hand the performance of the bPSO approach is superior for low levels of noise (10 dB). Taking into account the high levels of noise encountered in ship hulls emphasis should be placed for the case of low SNRs. Therefore, the improvement of the detection system for these cases is very important.

TABLE II
TOTAL ACCURACY

	Number of Projection Directions			
	One (1)	Two (2)	Three (3)	Four (4)
Noise free	91.58	91.58	91.32	91.84
20 dB	86.93	84.80	84.27	83.73
10 dB	81.87	83.47	80.00	81.87
0 dB	81.37	79.45	75.34	74.79
-10 dB	75.38	68.72	68.97	66.41
-20 dB	67.02	65.74	60.43	63.62

TABLE III
GA VS. BPSO CLASSIFICATION SCHEME PERFORMANCE

	+10 dB	0 dB	-10 dB
bPSO	90.67	81.92	74.62
GA	83.47	81.37	75.38

V. CONCLUSIONS

In this research work, an efficient feature definition algorithm for continuous monitoring of AE events in the presence of additive white-Gaussian noise was presented. A robust set of features is derived giving satisfactory localization rates of a single event in very noisy environments. The proposed method can be used to define a set of features, which can be embodied in real-time crack monitoring systems of large and complex structures improving the performance reliability in noisy environment. From an industrial point of view, the development of fast and efficient monitoring machines can be easily achieved using a small number of features in low-cost hardware. The crack characterization rate of the extent of damage is promising; however, more work has to be done for accurate location of crack using fewer sensors.

The results show that the use of just one projection direction outperforms all other configurations for low SNRs. This is just another manifestation of the "parsimony principle". In future work the performance of the AE localization system will let different projections to be calculated for each of the sensors as well as projections that will treat all features in a unified manner (the projection vector will have a dimension of 360). Moreover, different classifiers will be evaluated to derive an effective combination of feature selection and classification method both in terms of generalization performance and computational complexity.

It must be noted that the differences in the ship-hull, ship size, construction materials etc. may influence the propagation behaviour of crack and crack growing signals, leading not necessarily to the same set of features for robust detection of AE events. This means that this method has to be tailored on the specific application. Nevertheless the methodology is generic enough to remain the same.

Special ultrasonic sensors must be installed, i.e. specifications of very low sensitivity in low frequencies (0-20KHz) have to be met, because most of real-noise sources in ships generate signals in this bandwidth (engine noise and sea waves). These types of noise can be easily eliminated using band-pass sensors. The sensors located in the side shell below the sea surface require high amplification because the sea absorbs significant part of the AE signal energy, as shown in this work.

APPENDIX

TABLE IV
NOISE- FREE CASE WITH 1 PROJECTION DIRECTION

		Predicted Class		
		A	B	C
True class	A	23.6	1	0.4
	B	0.2	19.4	2.4
	C	0.4	2	26.6

TABLE V
+20DB SNR CASE WITH 1 PROJECTION DIRECTION

		Predicted Class		
		A	B	C
True class	A	23	0.4	1.6
	B	0.8	20	1.2
	C	2.8	3	22.2

TABLE VI
+10DB SNR CASE WITH 1 PROJECTION DIRECTION

		Predicted Class		
		A	B	C
True class	A	22.6	0.2	2.2
	B	1.2	17.4	3.4
	C	3.8	2.8	21.4

TABLE VII
0DB SNR CASE WITH 1 PROJECTION DIRECTION

		Predicted Class		
		A	B	C
True class	A	19.6	1	3.4
	B	0.6	17	3.4
	C	2.2	3	22.8

TABLE VIII
-10DB SNR CASE WITH 1 PROJECTION DIRECTION

		Predicted Class		
		A	B	C
True class	A	19	1.6	3.4
	B	0.8	18.4	4.8
	C	4.2	4.4	21.4

TABLE IX
-20DB SNR CASE WITH 1 PROJECTION DIRECTION

		Predicted Class		
		A	B	C
True class	A	20.4	2.4	6.2
	B	3.6	17.8	6.6
	C	6.2	6	24.8

TABLE X
NOISE- FREE CASE WITH 2 PROJECTION DIRECTIONS

		Predicted Class		
		A	B	C
True class	A	24.2	0.6	0.2
	B	0.8	18.8	2.4
	C	1.6	0.8	26.6

TABLE XI
+20DB SNR CASE WITH 2 PROJECTION DIRECTIONS

		Predicted Class		
		A	B	C
True class	A	21.6	0.6	2.8
	B	0.2	19.2	2.6
	C	2	3.2	22.8

TABLE XII
+10DB SNR CASE WITH 2 PROJECTION DIRECTIONS

		Predicted Class		
		A	B	C
True class	A	21	0.8	3.2
	B	1.6	18.4	2
	C	1	3.8	23.2

TABLE XIII
0DB SNR CASE WITH 2 PROJECTION DIRECTIONS

		Predicted Class		
		A	B	C
True class	A	21.2	0.8	2
	B	0.8	16.4	3.8
	C	3.6	4	20.4

TABLE XIV
-10DB SNR CASE WITH 2 PROJECTION DIRECTIONS

		Predicted Class		
		A	B	C
True class	A	16.8	2.8	4.4
	B	1.2	18.2	4.6
	C	5.6	5.8	18.6

TABLE XV
-20DB SNR CASE WITH 2 PROJECTION DIRECTIONS

		Predicted Class		
		A	B	C
True class	A	20.6	3	5.4
	B	3.4	16	8.6
	C	6.4	5.4	25.2

TABLE XVI
NOISE- FREE CASE WITH 3 PROJECTION DIRECTIONS

		Predicted Class		
		A	B	C
True class	A	24	0	1
	B	0.6	18.8	2.6
	C	0.6	1.8	26.6

TABLE XVII
+20DB SNR CASE WITH 3 PROJECTION DIRECTIONS

		Predicted Class		
		A	B	C
True class	A	21.8	0.2	3
	B	0.4	19.2	2.4
	C	3.4	2.4	22.2

TABLE XVIII
+10DB SNR CASE WITH 3 PROJECTION DIRECTIONS

		Predicted Class		
		A	B	C
True class	A	20.8	1.2	3
	B	1.4	17	3.6
	C	2	3.8	22.2

TABLE XIX
0DB SNR CASE WITH 3 PROJECTION DIRECTIONS

		Predicted Class		
		A	B	C
True class	A	20.6	0.2	3.2
	B	1	15	5
	C	4.2	4.4	19.4

TABLE XX
-10DB SNR CASE WITH 3 PROJECTION DIRECTIONS

		Predicted Class		
		A	B	C
True class	A	19.4	0.6	4
	B	2.2	16.2	5.6
	C	3.6	8.2	18.2

TABLE XXI
-20DB SNR CASE WITH 3 PROJECTION DIRECTIONS

		Predicted Class		
		A	B	C
True class	A	4	16	8
	B	7.6	7.6	21.8
	C	19	4.4	5.6

TABLE XXII
NOISE- FREE CASE WITH 4 PROJECTION DIRECTIONS

		Predicted Class		
		A	B	C
True class	A	23.8	0.2	1
	B	0.2	19.4	2.4
	C	1.4	1	26.6

TABLE XXIII
+20DB SNR CASE WITH 4 PROJECTION DIRECTIONS

		Predicted Class		
		A	B	C
True class	A	22.4	0.2	2.4
	B	1.2	16	4.8
	C	1.2	2.4	24.4

TABLE XXIV
+10DB SNR CASE WITH 4 PROJECTION DIRECTIONS

		Predicted Class		
		A	B	C
True class	A	22.4	1	1.6
	B	1.8	17.6	2.6
	C	3.2	3.4	21.4

TABLE XXV
0DB SNR CASE WITH 4 PROJECTION DIRECTIONS

		Predicted Class		
		A	B	C
True class	A	18.8	1.2	4
	B	0.6	15.6	4.8
	C	3.2	4.6	20.2

TABLE XXVI
-10DB SNR CASE WITH 4 PROJECTION DIRECTIONS

		Predicted Class		
		A	B	C
True class	A	18	2	4
	B	3.2	14.2	6.6
	C	4.8	5.6	19.6

TABLE XXVII
-20DB SNR CASE WITH 4 PROJECTION DIRECTIONS

		Predicted Class		
		A	B	C
True class	A	19.6	4.2	5.2
	B	4.4	17.2	6.4
	C	7.8	6.2	23

REFERENCES.

[1] J. Spanner, *Acoustic emission-techniques and applications. Intex Publication Co*, Illinois, USA. 1974.

[2] R. Williams, *Acoustic emission*. A. Hilger, Bristol, 1980

[3] R. Strathaus, R. Bea, Fatigue database development and analysis. Technical Report SMP 1-1, Department of Naval Architecture & Offshore Engineering, University of California at Berkeley, 1992

[4] D. Sucharski, Crude oil tanker hull structure fracturing: An operator's perspective. *In Proceedings of the prevention of fracture in ship structure*. Washington D.C., pp 87-124, 1995

[5] I. Lotsberg, E. Landet, Fatigue capacity of side longitudinals in floating structures. *Marine Structures* 18: pp 25-24, 2005

[6] G. Soares, Y. Garbatov, Fatigue reliability of the ship hull girder accounting for inspection and repair. *Reliability Engineering and System Safety* 51: pp 341-351, 1996

[7] A. Zubaydi, M. Haddara, A. Swamidas, On the use of the autocorrelation function to identify the damage in the side of a ship's hull. *Marine Structures* 13: pp 537-551, 2000

[8] A. Zubaydi, M. Haddara, A. Swamidas, Damage identification in a ship's structure using neural networks. *Ocean Engineering* 29: pp 1187-1200, 2002

[9] I. Guyon and A. Elisseeff, “An introduction to variable and feature selection” *J. Machine Learning Research.*, vol. 3, pp 1157-1182, 2003.
[10] S. Theodoridis and K. Koutroumbas, *Pattern Recognition*, 4th edition, Academic Press, 2008.
[11] V. Kappatos and E. Dermatas, “Feature extraction for crack detection in raining conditions”. *Journal of Nondestructive Evaluation* 26: 57-70, 2007.
[12] V. Kappatos, G. Georgoulas and E. Dermatas, "Crack Characterization in Ship Hulls Based on Features Selected Using the Binary Particle Swarm Algorithm", *Proc. of the 8th HSTAM International Congress on Mechanics,* Patras, Greece, July 12-14, 2007
[13] M. L. Raymer, W. F. Punch, E. D. Goodman, L. A. Kuhn and A. K. Jain, “Dimensionality reduction using genetic algorithms,” *IEEE Trans Evolutionary Computation,* vol 4, no 2, pp 164-171, July 2000
[14] Z. Sun, G. Bebis, X. Yuan and S. J. Luis, “Genetic feature subset selection for gender classification: a comparative study” *IEEE Workshop on Applications of Computer Vision*, 2002
[15] A. Nielsen *Acoustic Emission Source Based on Pencil Lead Breaking*. The Danish Welding Institute Publication, 1980
[16] GEATbx - The Genetic and Evolutionary Algorithm Toolbox for Matlab http://www.geatbx.com/
[17] T. Back, *Evolutionary algorithms in theory and practice*, Oxford University Press 1996.
[18] J. E Baker. “Reducing Bias and Inefficiency in the Selection Algorithm”. *In Proceedings of the Second International Conference on Genetic Algorithms*, pp. 14-21, 1987.
[19] H. Mühlenbein, and D. Schlierkamp-Voosen, “Predictive Models for the Breeder Genetic Algorithm: I. Continuous Parameter Optimization. *Evolutionary Computation*, vol 1, no 1, pp. 25-49, 1993.
[20] M J. P. de Sa. *Pattern recognition. Concepts, methods, and applications*, Springer, 2001